

# An Analysis of the Natural Circulation Pattern of the Supercritical Water Reactor based on the Thermohydraulic Properties

**Milad Mansouri Rad**

Received: 08 July 2019 / Received in revised form: 17 November 2019, Accepted: 23 November 2019, Published online: 25 January 2020  
© Biochemical Technology Society 2014-2020  
© Sevas Educational Society 2008

## Abstract

Supercritical water-cooled reactors (SCWR) are one of the six types of nuclear reactors proposed by the Generation IV International Forum (GIF), which are basically light water reactors (LWR). SCWRs are specifically designed to remove heat from the core using the natural circulation system, a routine which is usually done by active pumps, while making the reactor functions safer. Since the conditions in the quasi-critical region are complicated for fluid like water, and the results of experiments and analyzes indicate discontinuities or extreme changes in various physical properties of water, the employed model tries to study the thermo-hydraulic properties and mass fluxes in the transient state. The computational model begins with the determination of the conservation equations (mass, energy, and momentum) for the nodes considered. In the model of the study of thermo-hydraulic properties, the discretization operations are performed after the formulation of conservation equations. Steady-state equations are next solved. Then, in order to investigate the mass flux in the transient conditions of the constant solution, we observe the mass flow fluctuation and fluctuations with the dependence of the mass flux on time.

**Key words:** Supercritical Water Reactor, Hydro-Thermal Properties, Conservation Equations

## Introduction

### *Natural circulation with super-critical water*

The natural flow refers to the transfer of fluid within a closed cycle, without the need to design an initial actuator, due to the gradient of density along the pathway under the influence of volumetric force. (Mollendorf and Gebhart, 1973). A natural circulation system proposes mathematical equations, energy, and the mode of transmission. The difference in density can occur both by introducing a lighter phase in the main fluid and by temperature division between complementary energy interactions with the surrounding environment in different parts of the path. Then, proper conditions for transferring energy from the high-temperature source to low-power sources without direct contact should be generated. The warmer fluid can get up from the source and reach the cold source. Given the buoyancy force, it returns to the cold material to prepare for stacking energy. Therefore, the fact that the cold source is at the top and the hot source is at the bottom is mandatory and natural. (Chen and Iwamoto, 2017) This simplicity is appropriate for any physical system in the structure, and improves reliability due to the removal of the fluid handler. This issue facilitates the operations of natural circulation system in engineering initiatives, as the basic concepts of the natural circulation system and its extensive applications are both widely studied. The supercritical circulation system can be considered as a new concept. During the last 15 years, important theoretical and experimental researches have only been carried out to propose controversial theories regarding system performance on the thermohydraulic and sustainability aspects. Because of the lack of comprehensiveness, the reported observations are hard to understand for novices.

### *Conservation equations for the system of thermohydraulic properties*

---

**Milad Mansouri Rad**

Physics and Energy Engineering Department, Amirkabir University of Technology (Tehran Polytechnic)

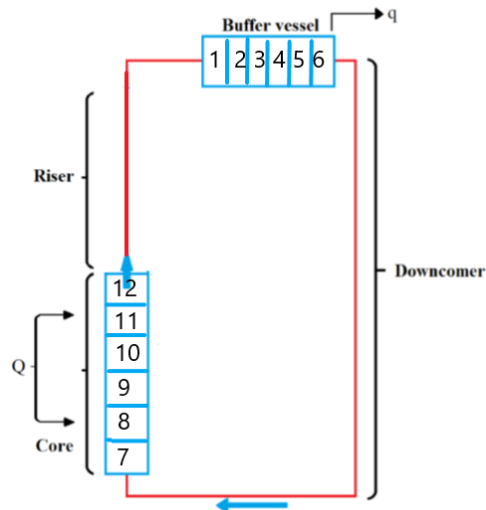


Figure 1: Model of water loop

In the above scheme system of natural circulation in many nodes with help of MATLAB and Relap5/3 designated and have had shown .

First we start with the mass equation, then the energy equation is expressed and finally we arrive at the momentum equations. In this model, the core and buffer, each contains six nodes. The length of the nodes remains constant.

$$\frac{\partial}{\partial t}(\rho V) + \frac{\partial}{\partial z}(\rho Av) = 0 \tag{1}$$

The aforementioned equation expresses the equation of mass. In general, when heated, the water enters the buffer through the up-lift flow and then returns to the heater through the down-lift. The mass equation that is written only includes the core and buffer, since the upward and downward velocities have geometric and, since there is no heat loss and heat transfer to the external environment, the downward and upward mass relations neutralize each other.

$$\frac{d(\rho Ae)}{dz} + \frac{d(\rho Ave_f)}{dz} = \begin{cases} P_h q_w \text{ for heater} \\ 0 \text{ adiabatic pipe} \\ -P_h q_w \text{ for hcooler} \end{cases} \tag{2}$$

In the energy equation, the right-hand side is designated with a negative sign for a cooler (buffer) indicating the loss or removal of heat. As in the adiabatic state, the right-hand side is considered to be zero due to the lack of heat transfer.

$$e_f = h_s + v^2/2 + gz \tag{3}$$

The above equation describes the energy equation in which  $e_f = p/\rho$ . The method adopted is based on constant thermal flux in the heater and buffer.

In other words, a positive flux is entered in the heater section, while a negative flux is introduced in the buffer section.

$$\frac{\partial}{\partial t}(\rho Av) + \frac{\partial}{\partial z}(\rho Av^2) = -A \frac{\partial P}{\partial z} - \tau_w P_w - \rho Ag \tag{4}$$

Then the momentum equations are expressed so that we can get the main output, i.e. the pressure.

All of the above equations depend on the external parameters for example Reynolds number, Nusselt number.

*The structure of the solving and implementation of the model of the study of thermohydraulic properties*

As previously mentioned, the conservation equations should be first discretized and then solved in the steady-state. If we intend to solve the problem in a transient phase, the introduction of disruption is necessary. In fact, the parameters that we need to consider are linear or

non-linear time independent or time-dependent disturbances. After entering the disturbances for the desired parameter, we solve it at the time to see the desired changes over time.

## Finite Difference Method

The finite difference is the mathematical expression of  $f(x + b) - f(x + a)$ . If a finite difference is divisible by  $(b-a)$ , then we will have a differential quotient.

In general, there are three commonly used forms for finite difference: forward, backward, and central differences. In this research, backward difference is utilized.

Its relation takes different forms according to the order.

First Order:

$$\Delta_h[f](x) = f(x+h) - f(x) \quad (5)$$

Second Order:

$$f''(x) \approx \frac{\Delta_h^2[f](x)}{h^2} = \frac{f(x+2h) - 2f(x+h) + f(x)}{h^2} \quad (6)$$

Solution: As we know from the definitions, the finite difference method is used for the discretization of the equations. These relationships are given below.

$$\rho_{i+1} A_{i+1} v_{i+1} = \rho_i A_i v_i \quad (7)$$

The above equation is in fact the relation of the conservation of the mass, which has taken the aforementioned form after discretization. Given that the cross-section is constant, by knowing the density and velocity of node  $i$ , the velocity and density of node  $i+1$  can be determined as follows:

$$(e_f)_{i+1} - (e_f)_i = \frac{1}{2} \left[ \left( \frac{q_{wPH}}{\rho A v} \right)_i + \left( \frac{q_{wPH}}{\rho A v} \right)_{i+1} \right] (z_{i+1} - z_i) \quad (8)$$

The above equation is derived from the discretization of the energy equation. If the parameters of the heat conduction, heated environment, density, cross-section, and velocity in the previous nodes are known, the enthalpy output can be calculated.

Finally, the momentum equation should be discretized, which takes the following form:

$$P_i - P_{i+1} = \frac{1}{2} \left( \frac{1}{A_i} + \frac{1}{A_{i+1}} \right) \left[ (\rho A v^2)_{i+1} - (\rho A v^2)_i \right] + \frac{1}{2} [\{\rho(F+g)\}_i + \{\rho(F+g)\}_{i+1}] (z_{i+1} - z_i) \quad (9)$$

$$\text{Where } F = \frac{\tau_w P_w}{\rho A}$$

As can be seen, the pressure output is determined from the above relation. First, let's consider the coefficient  $F$ , i.e. the pressure drop to be constant. The introduction of the Yamashita and Popov pressure drop coefficients makes the conditions more realistic.

By obtaining these equations and paying attention to the necessary details for solving these problems, the suitable outputs are achieved.

The formulation of pseudo-codes for these calculations includes the constants that should be considered at the beginning of the code-writing process. Thermo-hydraulic variables are then added. Next, the initial values that are to be changed throughout the system are introduced. The inputs of the problem, i.e. heat and thermal power are finally introduced.

Now we have to introduce the general framework for the formulas: How heat enters the system and how it gets out of the system; How the nodes are formulated and what are the constraints leading to the convergence of the solution of the equations?

Once the framework of the equations has been established, we must obtain the appropriate results as output. Several separate codes are written for the study of thermo-hydraulic properties, but the general principles are as described above.

*Obtaining steady-state values*

To investigate the thermohydraulic properties, the conservation equations of the system are discretized with a finite difference method, then solved by the forward variation method. This solution is based on the constant thermal flux in the heater and buffer sections, by which the inputs of the problem and the fixed and variable values are determined. Thus, the output pressure is determined from the momentum equation; the enthalpy is obtained from the energy equation; and density, and mass flux are determined from the mass equations. To solve the nonlinear equations of mass, energy and momentum, the boundary conditions are determined. In this research, the boundary conditions and equations are altered several times to yield the appropriate result. In some instances, the pressure drop has been considered constant while in others, it was introduced as a variable. A special consideration should be made to calculate the steady-state values. In the proposed system for steady-state mapping, operational characteristics cannot be expressed explicitly. In fact, iterative calculations are made for parameters to determine conditions at any interval. The initial guesses for the iterative process are in fact equivalent to explicit expressions, but the characteristics in the WHILE loop are again set to compute a steady state flow, which relates to the dependency between the values of the steady state. In the code input section, a command is written to stop the loop procedure, so that the user can strike a balance between the accuracy and speed of the calculation. Several functions have been used for implementing the state equation for the specific volume, temperature and conductivity of the cooling coil. These functions require an enthalpy input parameter (which specifies the specific enthalpy of a specific node) to give the output volume of the special volume, temperature, and thermal conductivity. There is another function called enthalpy that requires a temperature input to yield an enthalpy as an output.

*Solution of the Steady State*

In the steady-state operations, all coefficients of time-derivative are zero. Parametric values at steady state are obtained from geometrical and operating conditions. For each point in the operation plan (including any operating conditions), a steady state position is specified. Steady-state parametric values are needed to perform the final stability analysis. From each previously stated conservation equation, there is a steady-state value for each time-dependent variable.

In the subcritical model, the steady state solutions are as follows:

$$\bar{H}_0 = H_{in} + \frac{Nu_0 \lambda_f P_{in} L (\bar{T}_w - \bar{T}_0)}{2WD_H} \tag{10}$$

$$\bar{T}_w = \frac{QD_H}{Nu_0 \lambda_f P_{in} L} + \bar{T}_0 \tag{11}$$

It should be noted that these solutions are interdependent. One might try to find independent analytic solutions based on approximations of the equation of state, but from the discussions that follow, we find that the numerical findings suffice.

The solutions to the conservation equations of the supercritical model are as follows:

$$L_0 = \frac{D_H W (h_{pc} - H_{in})}{Nu_0 \lambda_f P_{in} (\bar{T}_{w,0} - \bar{T}_0)} = \frac{D_H \bar{W} h_{pc} N_{sub}}{Nu_0 \lambda_f P_{in} (\bar{T}_{w,0} - \bar{T}_0)} \tag{12}$$

$$\bar{H}_1 = h_{pc} + \frac{Nu_1 \lambda_f P_{in} \bar{L}_1}{D_H \bar{W}} (\bar{T}_{w,1} - \bar{T}_1) \tag{13}$$

$$\bar{T}_{w,0} = \frac{Q \frac{\bar{L}_0}{L} + \frac{Nu_0 \lambda_f P_{in} \bar{L}_0}{D_H} \bar{T}_0 + \frac{2\lambda_w}{L} A_w \bar{T}_{w,1}}{\frac{Nu_0 \lambda_f P_{in} \bar{L}_0}{D_H} + \frac{2\lambda_w}{L} A_w} \tag{14}$$

$$\bar{T}_{w,1} = \frac{Q \frac{\bar{L}_1}{L} + \frac{Nu_1 \lambda_f P_{in} \bar{L}_1}{D_H} \bar{T}_1 + \frac{2\lambda_w}{L} A_w \bar{T}_{w,0}}{\frac{Nu_1 \lambda_f P_{in} \bar{L}_1}{D_H} + \frac{2\lambda_w}{L} A_w} \tag{15}$$

According to Eq. (12), the length of  $L_0$  may be equal to or greater than the total length of the core. This is, however, incompatible with the enthalpy model.

If  $L_0 = L_1$ , then  $L_1 = 0$ . It is concluded from equations (12) and (15) that  $N_{\Delta h} = N_{sub}$

In cases where  $N_{\Delta h}$  is smaller than  $N_{sub}$ , the subcritical model is established, while the opposite pertains to cases where the supercritical model is established.

## Results

### *Study of thermohydraulic properties of the system*

In order to study the various thermohydraulic properties of the system, the conservation formulas of mass, energy and momentum within the desired system are first established and then the discretization process is undertaken by finite difference method. A specific type of finite difference called the forward finite difference is used for this purpose. After discretization by the forward finite difference method based on the constant heat flux in the heater (core) and the cooler (buffer), the enthalpy, velocity and pressure input variables, and hence the outputs, are determined using steady state solution. The pressure output is obtained by solving the momentum equation. The velocity output is also obtained from the solution of the equation of mass and mass flux from this relation. In general, the model of how to modify these properties is derived from *XSteam*, a MATLAB input code, to express conditions well when moving from sub-subcritical to supercritical temperatures. As stated earlier, the system is assumed to have a pressure of 25 MPa (supercritical pressure or condensed area), whether the system is in a supercritical state or not is determined by the fluid temperature. If the temperature is above the critical point, the system is in a supercritical state. We now show the thermohydraulic properties of the system in the steady state according to the geometrical conditions of the channel as shown in the table below.

Table 1: Design parameters considered as reference in this analysis

Design Parameters	Value
Pressure	25 MPa
Hydraulic Diameter	14 mm
Channel cross-sectional area	0.153 m <sup>2</sup>
Gravitational acceleration	9.8

The following diagrams are obtained with respect to the above properties. These conditions are modified according to the type of analysis, if necessary, with relevant explanations.

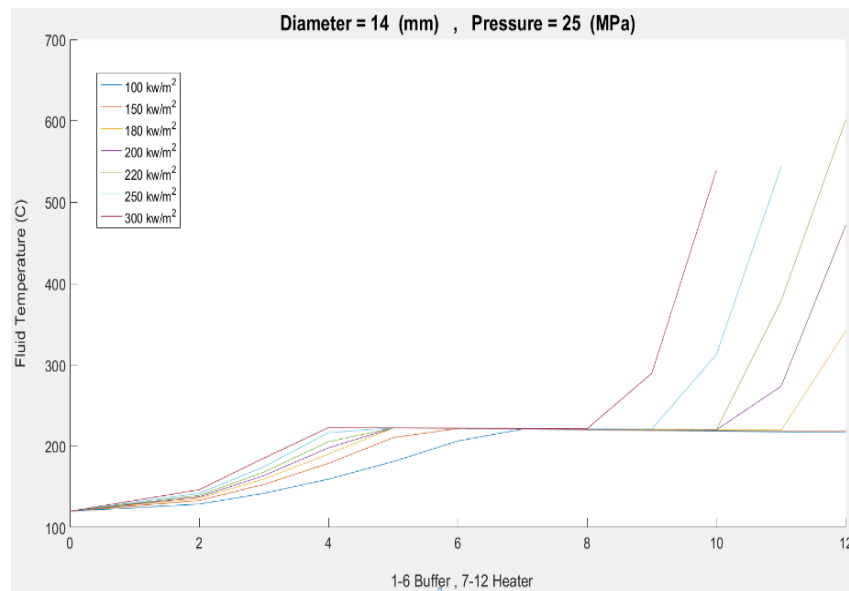


**Figure 1:** Diagram of fluid temperature at different points in the system at seven different heat fluxes

Figure 1 illustrates the fluid temperature along with the system. Since the uplifting and down-lifting sections act as fluid carriers and have no effect on thermo-hydraulic conditions, only buffer and heater positions are considered. This is what it really means when there is no heat transfer to the external environment like our system.

What immediately follows is the dramatic increase in temperature from the buffer section to the heater, which intensifies with increasing heat flux.

As we increase the thermal power, it is observed that the temperature increases as the temperature rises and reaches higher temperatures in the lower nodes. If the heat flux is not applied properly, our system will have a temperature below the critical temperature of 373.9 °C and the system will not become supercritical.

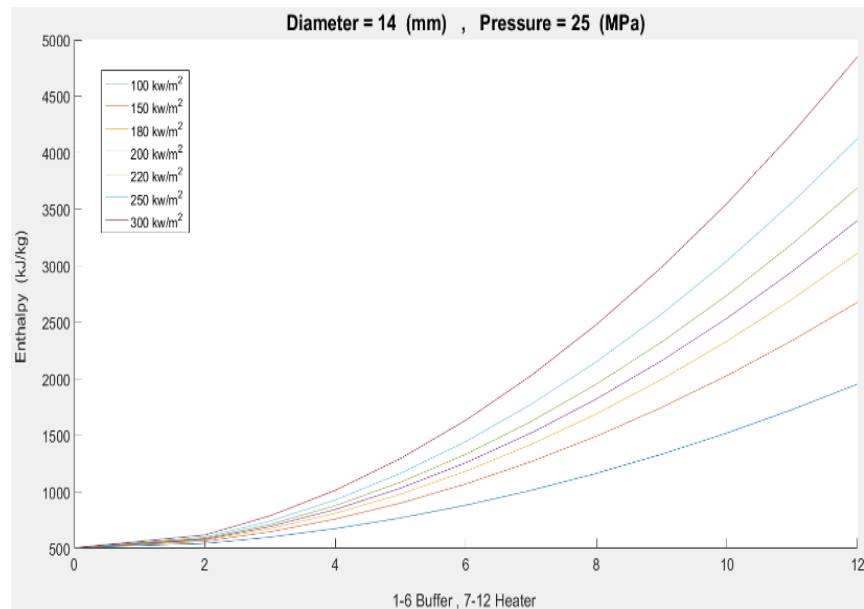


**Figure 2:** Diagram of fluid enthalpy at different points in the system at seven different heat fluxes

In Fig. 2, we observe that the fluid enthalpy increases as it passes through the heater. This increase occurs nonlinearly. As can be seen, the effect of thermal power is such that the system may never be supercritical at low flux.

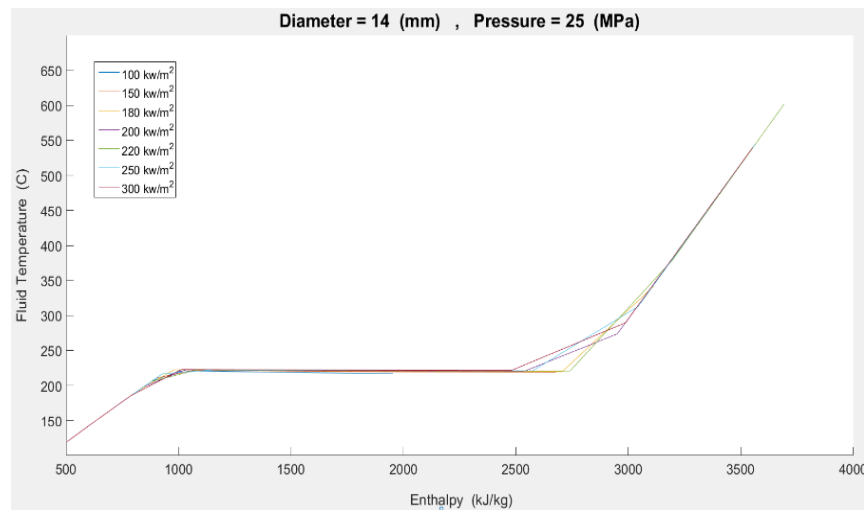


**Figure 3:** Flow temperature diagram in terms of system enthalpy at seven different heat fluxes

The fluid temperature against enthalpy is shown in Figure 3. The general trend is upwards, yet a turning point in the transition of the quasi-critical region is evident. According to the diagram, the system reaches supercritical temperature at low thermal powers as well. But the temperature jump is greater at higher power values. Figure 4 shows the enthalpy of temperature at a constant pressure of 25 MPa. The overall form is similar, but given the pressure drop and the equations that are considered, it differs from the actual data obtained from XSteam.

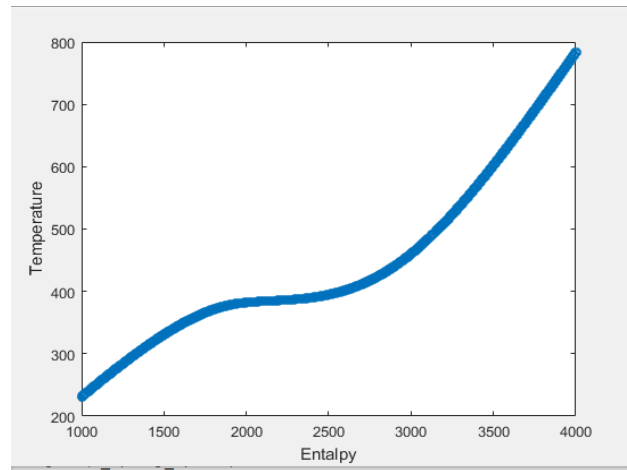


**Figure 4:** Temperature graph based on enthalpy at constant pressure of 25 MPa. Derived from XSteam code

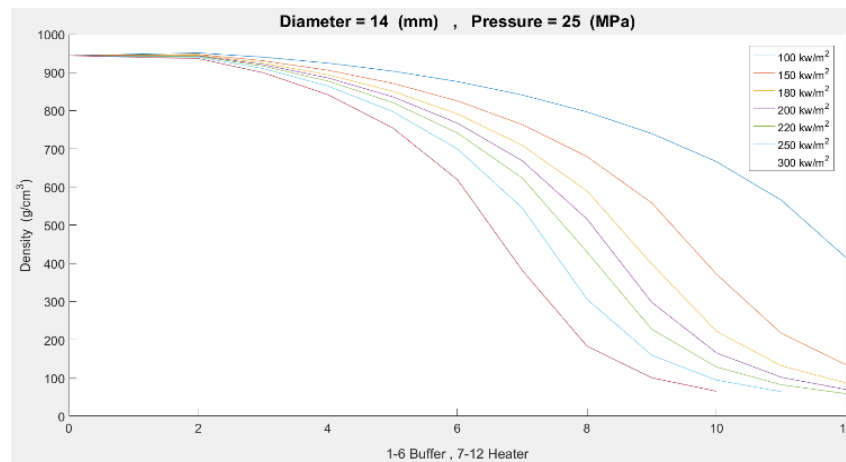


**Figure 5.** The fluid density of fluid in different points of the system in seven different thermal fluxes

Figure 5 shows the density of fluid at different points in the system. As the heat flux increases, the density decreases rapidly and reaches less than  $90 \text{ kg/m}^3$  in the lowest case. We should know that the density only decreases sharply in the sub-critical region, that is, when the system reaches the supercritical state, the fluid (water) density drops dramatically. We now turn to the issue of pressure drop after acquiring some important thermodynamic properties. Pressure loss in natural circulation cycle systems occurs in the form of gravitational pressure drop and frictional pressure drop. In this thesis, we examine the pressure drop caused by friction. There are various types of pressure drop relationships, but as discussed in Chapter 2, we use the best pressure drop relationships in supercritical systems and compare the results with the conventional Blasius and McAdams equations. The difference of these relations can be seen by obtaining the graph of pressure drop coefficients in terms of temperature. It should be noted, however, that these diagrams depend on specific conditions related to density, temperature difference, viscosity in volume fluid, and near the wall. We need to know if the diagrams are plotted depending on the temperature of the fluid near the wall. If there is no temperature difference between the two, we take the ratio of viscosities and densities equal to 1 and replace the equations. The following diagrams show the difference in the pressure drop relationship at  $210 \text{ (kg/m}^2\text{)}$  heat flux and the absence of difference between the bulk temperature and the fluid temperature near the wall.

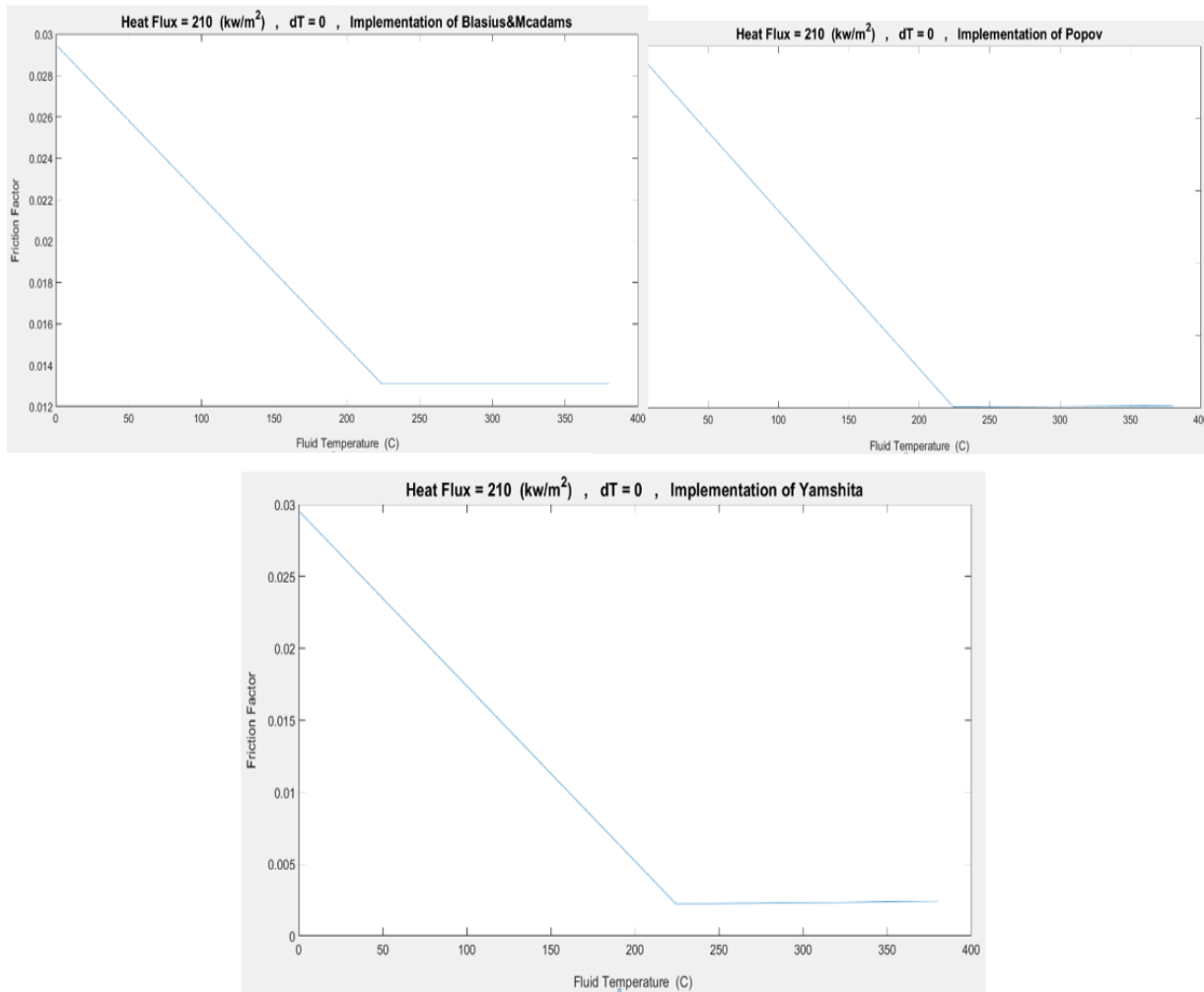


**Figure 6:** Diagram of different friction factors by temperature

As can be seen, the figures a, b, c show the relation of Blasius-McAdams, Yamshita and Popov respectively. Various differences are evident. The general trend is similar, but the Yamshita and Popov relations show closer values, with the lowest value in the Popov relation at 0.005 and in the Yamshita relation at 0.004, while for Blasius-McAdams, minimum occurs at 0.012. It should be noted that the values obtained at different input flows will also vary. It was previously stated that the friction factor relationship depends on the temperature difference between the bulk fluid and the fluid near the wall, so that if the temperature difference between the channel wall at which the heat is generated and the fluid inside the channel is zero, these formulas are greatly simplified. Then the ratio of viscosities and densities equals 1 and the equation is converted to an isothermal one. Our graphs are all isothermal. Graphs show predictable behavior. Due to the decrease in density and viscosity at high temperature points and reaching the quasi-critical area, the pressure drop coefficients also decrease. It should also be kept in mind that with decreasing density, if the charge is constant, the rate of increase causes the pressure drop to decrease further as the Reynolds number increases. If we look closely, we can see that if there is a positive and negative temperature difference between the fluid and the wall due to the temperature exchange, the differences before the sub-critical temperature reach the peak of the thermohydraulic properties differences and are significantly different from our diagram. It does. Finally, as we pass the quasi-critical region, the values approach the isothermal value again. First, by considering the pressure drop from the relationship between Blasius and McAdams, we obtain the following results:

$$\text{Blasius} \quad f = 0.316Re^{-0.25} \quad Re < 30.000$$

$$\text{McAdams} \quad f = 0.184Re^{-0.20} \quad 30.000 < Re < 10^6$$

The Reynolds number depends on several parameters with respect to the following relation. One of the effective parameters for our system is density and dynamic viscosity because the initial velocity is given and the length is constant. If changes in these two parameters are tracked throughout the system, one can see what parameter is effective in obtaining such a result for the Reynolds number.

$$Re = \frac{\rho u L}{\mu \nu}$$

(16)

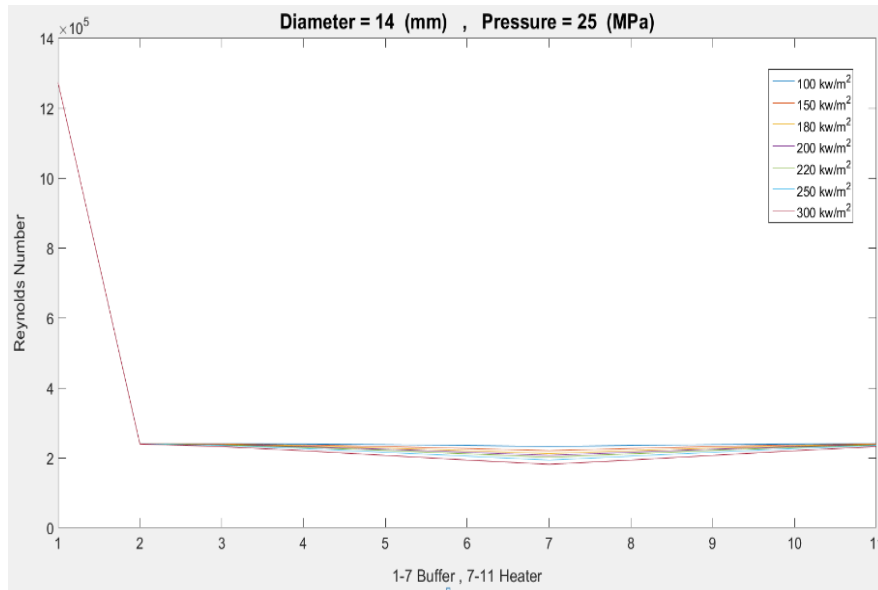
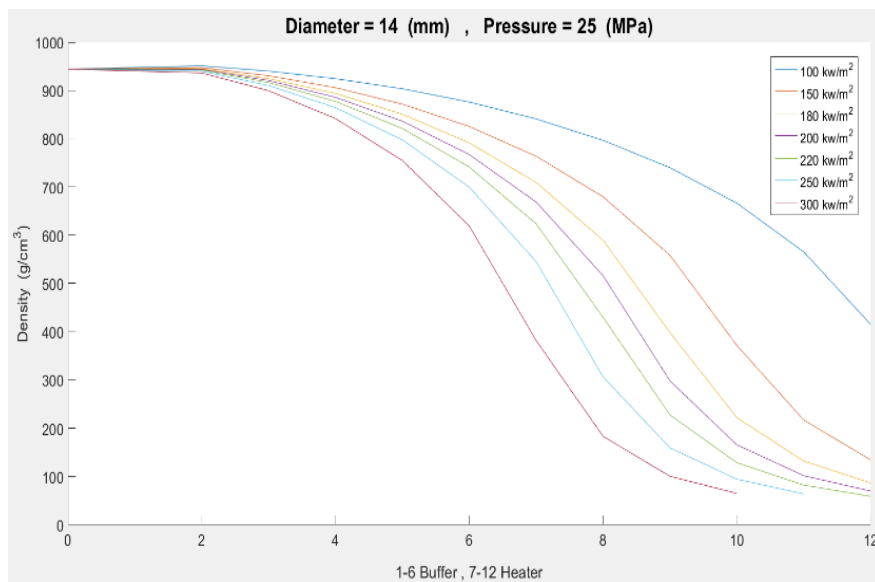
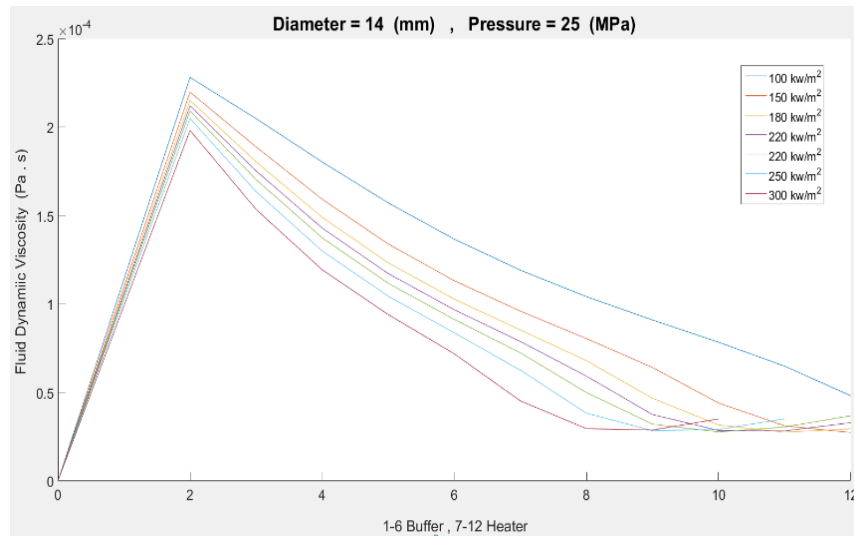


Figure 7: Diagram of Reynolds number variations at different points in the system at seven different heat fluxes





**Figure 8:** Diagram of dynamic viscosity changes at different points in the system at seven different heat fluxes

Based on the results and the position of these two parameters in the Reynolds relation, it is safe to say that the reason for the Reynolds decrease in the graph is owing to the relative density constant and the increase in dynamic viscosity at first. Then the Reynolds diagram shows approximately constant conditions, which is due to the decrease in both density and viscosity in the system. It should be noted that the viscosity diagram of the system is in the sub-critical region until the sixth node and the mild increase in the dynamic viscosity after the represents the system reaching supercritical conditions.

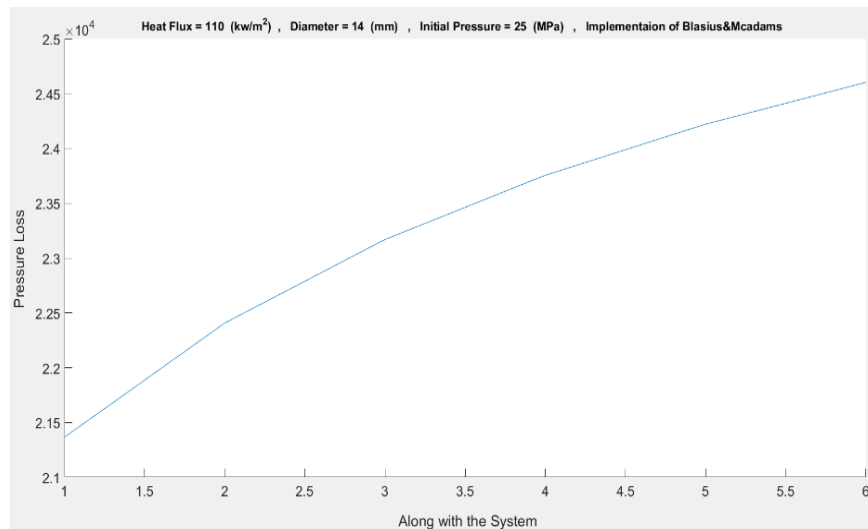


**Figure 9:** Diagram of pressure drop at various points of the system causing a drop in the constant heat flux of 110 kw/m<sup>2</sup>

By solving the momentum equation and applying the pressure drop coefficient of Blacius and McAdams, we obtain the output pressure as above.

Finally, after examining the diagrams in question using Blacius-McAdams coefficient, Yamshita pressure drop coefficient is introduced to the system.

This relation includes parameters that each may experience significant changes throughout the system. The following formula illustrates this:

$$f = f_{iso,b} \left( \frac{\mu_w}{\mu_b} \right)^{0.72}$$

$$f_{iso,b} = \frac{0.314}{0.7 - 1.65 \log Re + (\log Re)^2}$$

Influential parameters include Reynolds, dynamic viscosity of the wall, and bulk viscosity of the fluid.

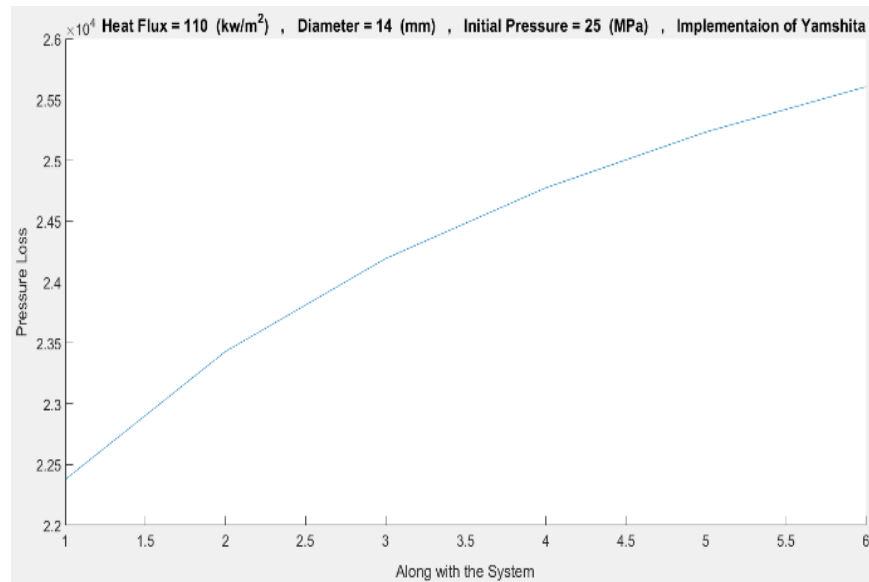


**Figure 10:** Diagrams of the Yamshita Relations

Comparing the results obtained by applying Yamshita's relation with that of Blasius and McAdams demonstrates the differences in the graphs, in the pressure diagram, the minimum pressure varies in two relations, as does the minimum and maximum pressure in final nodes.

$$f = f_{iso,b} \left( \frac{\rho_w}{\rho_b} \right)^{0.74}$$

$$f_{iso,b} = (0.79 \ln Re - 1.64)^{-2}$$

We now apply Popov's relation.

Popov's pressure drop formula is as follows:

$$f = f_{iso,b} \left( \frac{\rho_w}{\rho_b} \right)^{0.74}$$

$$f_{iso,b} = (0.79 \ln Re - 1.64)^{-2}$$

The influential parameters here are Reynolds number and density.

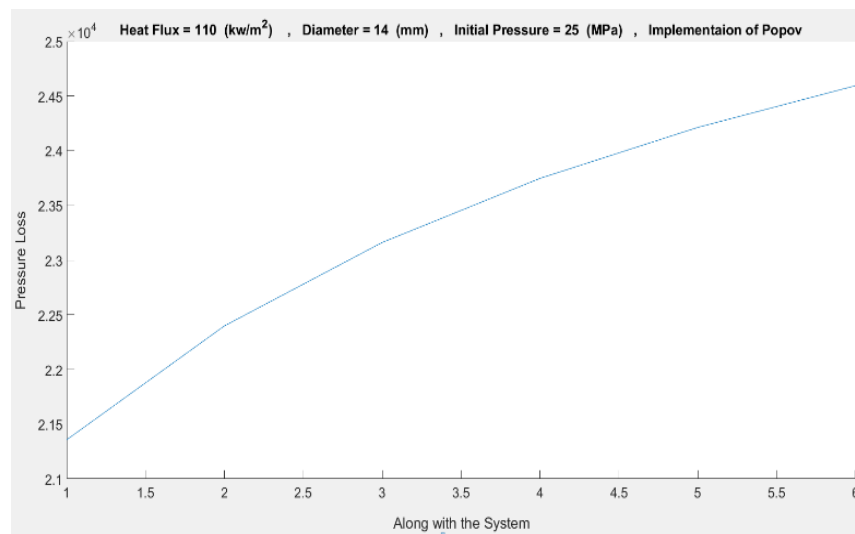


**Figure 11:** Pressure diagram along the system for applying Popov's relation

Considering the results, it is evident that these graphs provide results similar to those of the Yamashita relation, and their differences with the Blasius McAdams relation are similar to the Yamashita relation.

In fact, it can be concluded that the pressure drop that the Expansion Tank (Reservoir) has to compensate for varies in accordance with our calculations and under different conditions.

## References

- [1] - Chen, L., & Iwamoto, Y. (Eds.). (2017). *Advanced Applications of Supercritical Fluids in Energy Systems*. IGI Global.
- Mollendorf, J. C., & Gebhart, B. (1973). An experimental and numerical study of the viscous stability of a round laminar vertical jet with and without thermal buoyancy for symmetric and asymmetric disturbances. *Journal of fluid mechanics*, 61(2), 367-399.
- [2] - An experimental and numerical study of the viscous stability of a vertical laminar round jet with and without thermal buoyancy for symmetric and asymmetric disturbances. November 1973, pp. 367-399
- [3] - Lin chen, Yuhiro Iwamoto. *Advanced supercritical Fluid application in Energy systems* .2017
- [4] T. Yamashita, H. Mori, S. Yoshida, and M. Ohno. Heat transfer and pressure drop of a supercritical pressure uid owing in a small diameter tube. *Memoirs of the Faculty of Engineering, Kyushu University*, 63 (4): 227244, 2003Energy systems .2017
- [5] – Ojefua Osazuwa Gabriel, Amidu Muritala Alade, Yehwudah E.Chad-Umoren,Science and Technology of Supercritical Water Cooled Reactors: Review and Status, Centre for Nuclear Energy Studies, University of Port Harcourt, PMB 5323, Port Harcourt, Nigeria
- [6] – M. K. S. Sarkar, . K. Tilak, and . N. Basu, “ state-of-the-art review of recent advances in supercritical natural circulation loops for nuclear applications,” Ann. Nucl. Energy, vol. 73, pp. 250– 263, 2014.